

Dual Path Transformer with Partition Attention

Zhengkai Jiang¹ Liang Liu¹

Jiangning Zhang¹ Yabiao Wang¹ Mingang Chen² Chengjie Wang¹

¹Tencent Youtu Lab, ²Shanghai Development Center of Computer Software Technolog

{zhengkaijiang, caseywang, jasoncjwang}@tencent.com

Abstract

This paper introduces a novel attention mechanism, called dual attention, which is both efficient and effective. The dual attention mechanism consists of two parallel components: local attention generated by Convolutional Neural Networks (CNNs) and long-range attention generated by Vision Transformers (ViTs). To address the high computational complexity and memory footprint of vanilla Multi-Head Self-Attention (MHSA), we introduce a novel Multi-Head Partition-wise Attention (MHPA) mechanism. The partition-wise attention approach models both intra-partition and inter-partition attention simultaneously. Building on the dual attention block and partition-wise attention mechanism, we present a hierarchical vision backbone called DualFormer. We evaluate the effectiveness of our model on several computer vision tasks, including image classification on ImageNet, object detection on COCO, and semantic segmentation on Cityscapes. Specifically, the proposed DualFormer-XS achieves 81.5% top-1 accuracy on ImageNet, outperforming the recent state-of-the-art MPViT-XS by 0.6% top-1 accuracy with much higher throughput.

1. Introduction

In recent years, attention mechanisms [45] and Transformers [26] have emerged as powerful tools for architecture design. The use of Transformers, such as Vision Transformers (ViTs) originally introduced in natural language processing (NLP) [14], has become prevalent in architecture design for a variety of computer vision tasks due to their powerful long-range dependency modeling ability. Recent research [31, 13, 27, 56] on Transformers has demonstrated promising performance on various computer vision tasks, including image classification [26], object detection [38, 8, 29, 24, 21, 23, 22], and semantic segmentation [33, 5].

Despite the remarkable success of visual transformers on various benchmarks, there still exist several challenges. The self-attention mechanism used in transformers results

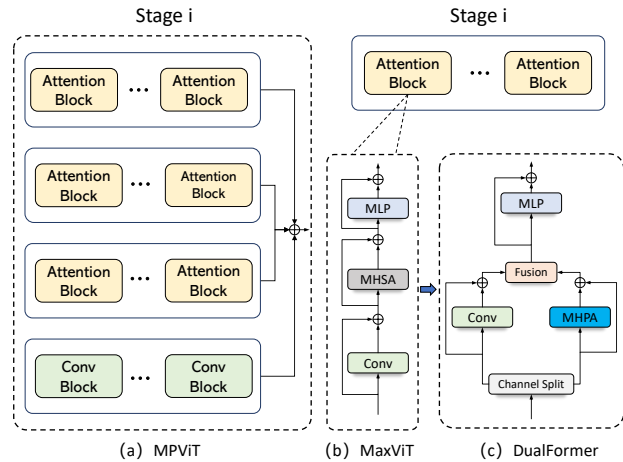


Figure 1. Comparison with recent ViT architectures, such as MPViT [27], which employs a stage-wise multi-path architecture in parallel, MaxViT [44], which stacks MBCConv [39] and self-attention blocks in series, and our proposed DualFormer, which efficiently combines partition-wise attention and MBCConv blocks through a dual-path design.

in quadratic computational and memory complexity, which limits their generalization on high-resolution images, particularly for dense prediction tasks such as object detection and semantic segmentation. To address this issue, several works propose self-attention variants, such as window attention [31], which is less effective to capture long-range dependencies, token selection [13, 52], which relies on the heuristic rules and replacing early-stage self-attention with depth-wise convolution blocks [15, 28] endowing local structure perception, which lacks long-range dependencies ability for low-level stages. Building upon previous work that has identified the existence of redundancy dependencies, as demonstrated in [2], and qualitative visualization seen in 4, we propose a novel technique called partition-wise attention that aims to achieve a balance between model performance and efficiency. The proposed method generates spatial partitions by clustering the feature representation level’s similarity. Within each partition, the self-attention mechanism is performed, resulting in higher

efficiency and a lower memory footprint. To enable the model to capture long-range dependencies, we also introduce inter-partition attention.

Besides the efficiency issue, the ability to model multi-scale or multiple receptive fields is another crucial factor for downstream tasks. To endow visual transformers with multi-scale modeling ability, CoaT [56] proposes the co-scale mechanism, which represents fine and coarse features simultaneously. Similarly, MPViT [27] introduces stage-wise multi-transformer paths in parallel to exploit multi-scale feature representation. However, both methods require heavy computation and memory overhead. In this paper, we propose *DualFormer*, a simple and efficient *dual path attention* mechanism to capture different scales and receptive field information through a novel approach. Our method first splits features along the channel dimension and then integrates the depth-wise convolution block and the proposed Multi-Head Partition-wise Attention (MHPA) in parallel before feeding them into the Feed-Forward Network (FFN) block. As illustrated in Fig 3, DualFormer comprises several patch embeddings and dual attention blocks. Each dual attention block consists of a convolution branch that captures local-wise feature dependencies and a self-attention branch that captures global feature dependencies in parallel. The features from both branches are then aggregated to enable both fine and coarse feature representations.

To demonstrate the effectiveness and efficiency of our proposed method, we conducted experiments on various tasks, including image classification on ImageNet-1K dataset, object detection on the MSCOCO dataset, and semantic segmentation on ADE20K. Specifically, our DualFormer-S model, which has 22.6M parameters and 4.4G FLOPs, achieved 83.5% top-1 accuracy for ImageNet-1K classification, 48.6% mAP for MSCOCO object detection, and 48.6% mIoU for ADE20K semantic segmentation. Our experiments demonstrate that DualFormer significantly outperforms state-of-the-art methods across different visual tasks

The main contributions are summarized as follows:

- Dual Path Vision Transformer (*DualFormer*) is proposed to simultaneously model various scales and receptive fields information, resulting in a more discriminative and detailed representation.
- To address the complexity and memory issues associated with the standard self-attention block, we propose performing self-attention within each group partition and cross-attention in a group-wise mechanism to model long-range dependency.
- Our proposed DualFormer achieves new state-of-the-art performances on a variety of vision tasks, includ-

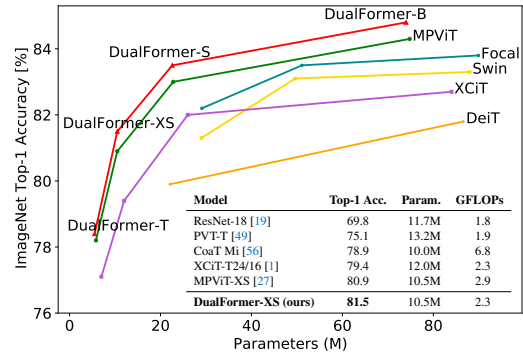


Figure 2. **Parameters vs. ImageNet Accuracy.** DualFormers outperform state-of-the-art Vision Transformers while having fewer parameters and FLOPs. The model names, T, XS, S, and B, denote tiny, extra-small, small, and base, respectively.

ing image classification, object detection, and semantic segmentation.

2. Related Work

2.1. Transformers for Vision

Transformers have recently achieved remarkable success in visual recognition [14, 31], becoming the de-facto standard in natural language processing tasks. ViT [14], as the pioneering work that introduced Transformers into vision tasks, applies a standard Transformer to images by splitting an image into patches and providing the sequence of linear embeddings of those patches as input to a Transformer, achieving state-of-the-art performance on image classification tasks. DeiT [43] introduces a distillation token mechanism that achieves competitive performance when trained only on ImageNet-1K with no external data. In addition to pure Transformer architectures, many researchers have explored combining CNNs and Transformers [15, 54, 9, 28, 37]. Container [15] unifies CNN and Transformer in a spatial context aggregation manner and further proposes to replace early-stage Multi-Head Self-Attention (MHSA) with convolutions, exploiting the inductive bias of local convolutions in shallow layers and leading to faster convergence speeds. Similarly, Uniformer [28] adopts a similar approach to Container, stacking convolutions in shallow layers and self-attention in deep layers, addressing both redundancy and dependency for efficient and effective representation learning. Many works [54, 37] follow the paradigm of inserting convolutions in the early stage, which increases optimization stability and convergence speed, together with better performance. However, the quadratic complexity of Transformers still remains intractable for high-resolution images, particularly for dense prediction tasks such as object detection and semantic segmentation.

2.2. Efficient Self-Attentions

Since the image resolution of vision tasks is typically very high, developing an efficient self-attention scheme is critical. Recent works [31, 13] adopt the local self-attention mechanism and achieve global interaction through shifted windows scheme to reduce the quadratic complexity of Transformers. Efficient Attention [40] proposes a novel efficient self-attention mechanism by switching the order of query, key, and value, resulting in substantially lower memory and computational costs. Performer [6] proposes a novel fast attention approach based on positive orthogonal random features with linear complexity. SOFT [35] replaces the original softmax operation in self-attention with a Gaussian kernel function, yielding dot-product similarity through low-rank matrix decomposition. XCiT [1] proposes modeling interactions across feature channels rather than tokens, resulting in linear complexity in the number of tokens. HamNet [16] formulates modeling global context as a low-rank recovery problem through matrix decomposition, outperforming a variety of attention modules on both image classification and dense prediction tasks with linear complexity. Flash Attention [10] proposes an IO-aware exact attention algorithm using tiling to reduce the number of memory reads and writes, resulting in a dramatic speedup on the long-range sequence and better performance. In this paper, inspired by GCNet [2] which shows that global contexts modeled by non-local networks are nearly the same for different query positions, we propose partition attention with a semantically dynamic group mechanism, discarding full self-attention, leading to high efficiency, especially for large resolution input images in object detection and semantic segmentation.

2.3. Combination of CNN and ViT

Another topic related to our work is the integration of Vision Transformers (ViT) and Convolutional Neural Networks (CNN) for general architecture design. Previous studies [15, 28, 36] propose replacing self-attention in shadow layers with convolution, rather than combining them. CeiT [60] suggested using image-to-tokens to generate low-level features with convolutions, which enhances the locality and long-range dependency modeling of Transformers. CMT [17, 13] introduced depth-wise convolution into the feed-forward network to encode local features. CvT [50] utilized convolutional token embedding before each stage and convolution projection of Transformer blocks. Subsequent works [54, 9] combined convolution into early stage of transformers for improved generalization and scalability. MPViT [27] proposes to use stage-wise multi-scale patch embeddings to exploit multi-scale and multi-path representation but accompanying high computational complexity. Inception Transformer [41] presents an inception mixer with high- and low-frequency paths based

on a hand-crafted channel-splitting manner. The most related work is ACMix [36] combining traditional convolution and self-attention in a hybrid way. However, both the self-attention branch and the convolution branch rely on the projected queries, keys, and values features with 1×1 convolutions. Inspired by HRNet [47] success, we instead design parallel convolution and attention branch mechanisms to exploit different frequencies and various scales representation, leading the more discriminative features with better performance and higher efficiency.

3. Method

Vanilla self-attention has quadratic computational and memory complexity with respect to input resolution, which hinders its use for dense prediction tasks such as object detection and semantic segmentation. To address the efficiency issue of self-attention, we propose an alternative partition attention with a dynamic token group mechanism. This mechanism can model global dependencies with high efficiency. Additionally, to reduce the computational complexity of shadow layers of partition attention, we adopt stride depth-wise convolution to downsample the input resolution. Recent studies [44, 63, 57, 59, 13] on transformer architecture design have adopted the paradigm of serially stacking global self-attention and local convolution. Inspired by the success of the multi-path and multi-scale in HRNet [46] and Inception Network [41], we propose a dual-path design that performs attention and local convolution in parallel, which allows for various scale modeling to obtain more discriminative feature representations.

In this section, we first present the architecture of our proposed DualFormer. Next, we provide a detailed explanation of partition-wise attention, following a brief review of the most typical multi-head self-attention, which comprises four components: the *partition generator*, *intra-partition attention*, *inter-partition attention*, and *local-global aggregation*. We then discuss various approaches to combining convolution and attention. Lastly, we provide a detailed description of the different configurations of the proposed DualFormer.

3.1. Overall Architecture

The overall architecture of the proposed DualFormer is depicted in Fig 3. Given an input image with a resolution of $H \times W \times 3$, we follow previous works [15, 28, 31] and employ two successive overlapped convolutional token embedding layers (3×3 convolution layer with stride 2) to obtain $\frac{H}{4} \times \frac{W}{4}$ patch tokens with a dimension of D . The entire network comprises four stages that generate a hierarchical representation for downstream dense prediction tasks. For each stage $i \in 1, 2, 3, 4$, DualFormer consists of N_i sequential *Dual Attention Blocks* while keeping the number of tokens constant. For the i^{th} stage, the feature maps have

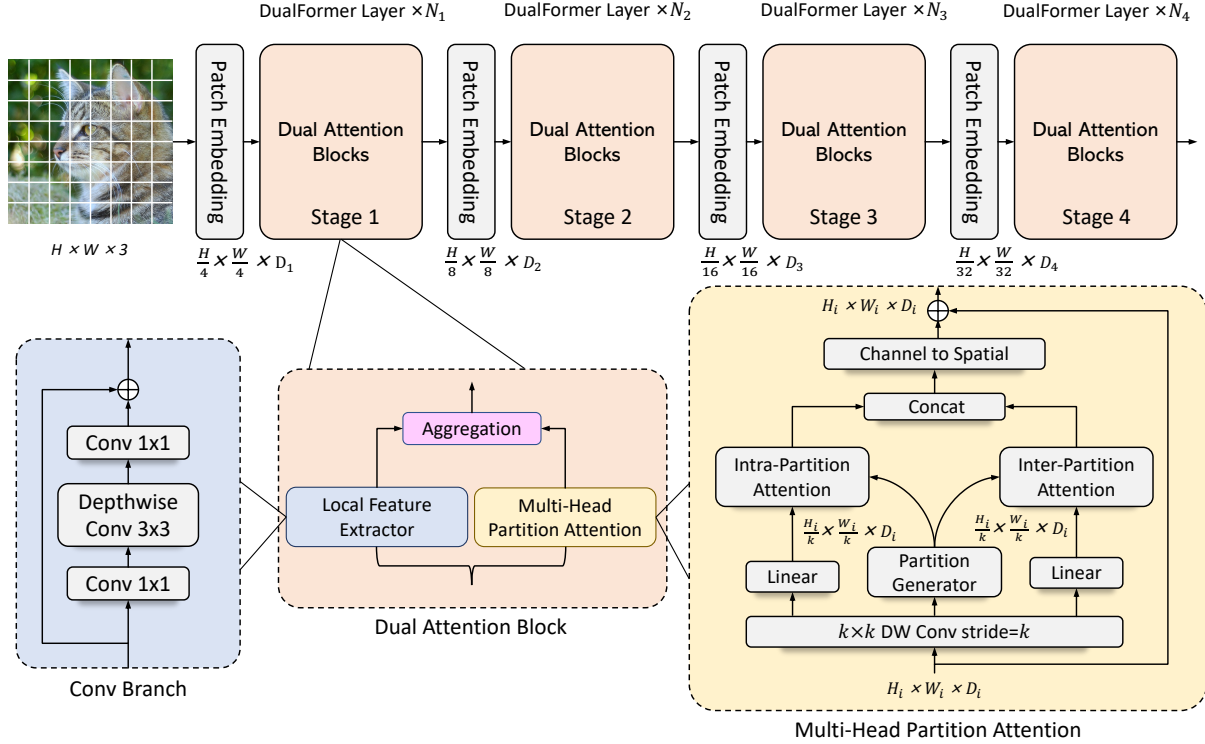


Figure 3. **DualFormer architecture.** We adopt a typical hierarchical design, similar to previous works [27, 31, 48], based on a proposed basic building block called the Dual Attention Block. This block unifies partition-wise attention and local feature extraction and generates four stages of features for downstream dense prediction tasks. To extract local features, we employ the MBCConv block [39], which uses depth-wise convolution to capture local spatial interactions. The Multi-head Partition Attention (MHPA) generates different spatial partitions first and then performs intra-partition and inter-partition attention, which are fused to generate fine-grained global interaction features. To reduce the computational complexity, MHPA utilizes depth-wise stride convolution to downsample the input resolution and recovers the original resolution via a channel-to-spatial mechanism.

$\frac{H}{2^i+1} \times \frac{W}{2^i+1}$ tokens, which is similar to both CNN backbones like ResNet [19] and prior Transformer backbones like Swin [31]. For image classification tasks, we use global average pooling from the last stage and feed it to the classification head. For dense prediction tasks, such as object detection and semantic segmentation, all four stages of feature maps are fed into the task head.

3.2. Approximating Attention with Clustering

Review Self-Attention. Given a set of n token sequence $\mathbf{X} \in \mathbb{R}^{n \times d}$ with d -dimensional vector for each token, self-attention [45] aims to compute a weighted sum of the values based on the affinity of each token. Mathematically, it can be formulated as follows:

$$\mathbf{Q} = \mathbf{X}\mathbf{W}_q, \mathbf{K} = \mathbf{X}\mathbf{W}_k, \mathbf{V} = \mathbf{X}\mathbf{W}_v, \quad (1)$$

where $\mathbf{W}_q \in \mathbb{R}^{d \times d_e}$, $\mathbf{W}_k \in \mathbb{R}^{d \times d_e}$, and $\mathbf{W}_v \in \mathbb{R}^{d \times d_e}$ are learnable projection weights. The query-specific attention maps $\mathbf{A} = \frac{\mathbf{Q}\mathbf{K}^T}{\sqrt{d_e}} \in \mathbb{R}^{n \times n}$ can be obtained by the scaled dot-product of \mathbf{Q} and \mathbf{K} . The whole global aggregation

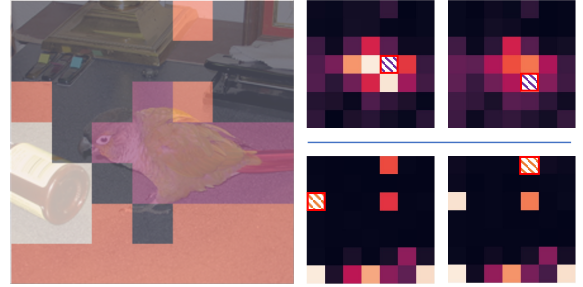


Figure 4. Visualization of attention maps for various query positions (indicated by red boxes) in a self-attention block on ImageNet validation set. The original image (shown on the left) is blended with a grouping result based on the feature map. It was observed that different queries within the same group exhibit similar attention maps.

operation can be formulated as:

$$\text{Attention}(\mathbf{Q}, \mathbf{K}, \mathbf{V}) = \text{softmax}\left(\frac{\mathbf{Q}\mathbf{K}^T}{\sqrt{d_e}}\right)\mathbf{V}. \quad (2)$$

Through an analysis of the attention weights of a ViT model pre-trained on ImageNet, as shown in Fig 4, we ob-

serve that the attention weights of different query locations are almost the same, indicating a large amount of redundancy. Thus phenomenon has also been observed in the GCNet [2]. To address this issue, we propose a clustering-based partition attention mechanism, which is a fast approximation of self-attention. Clustering-based partition attention masks use of similarities between queries and groups them to reduce the computational cost. It mainly comprises four modules: the Partition Generator, Intra-Partition Attention, Inter-Partition Attention, and Aggregation.

Partition Generator. Given flatten input feature map $x \in \mathbb{R}^{n \times d}$, we aim to group spatial locations into K distinct clusters defining the partition $\mathcal{C} = \{\mathcal{C}_k\}_{k=1}^K$, with $\cup_k \mathcal{C}_k = \{x_i\}_{i=1}^n$ and $\mathcal{C}_i \cap \mathcal{C}_j = \emptyset, \forall i \neq j$. Each cluster \mathcal{C}_k of the partition is represented by a centroid $\mu_k \in \mathbb{R}^d, \forall k \in \{1, \dots, K\}$. The goal is to find centroids minimizing the following error function:

$$\min_{\mathcal{C}, \mu_1, \dots, \mu_K} \sum_{k=1}^K \sum_{x_i \in \mathcal{C}_k} \mathcal{L}(x_i, \mu_k), \quad (3)$$

To assign $x_i \in \mathbb{R}^d, i \in 1, \dots, n$ to a cluster \mathcal{C}_k , we evaluate the similarity measure \mathcal{L} . Specifically, x_i belongs to the cluster \mathcal{C}_l if and only if $l = \arg \min_k \mathcal{L}(x_i, \mu_k)$. The Euclidean distance in terms of their \mathcal{L}_2 norm can be used as the similarity measure, i.e., $\mathcal{L}(x_i, \mu_k) = \|x_i - \mu_k\|_2^2$. To improve the efficiency of solving the optimization problem, we use the more efficient and GPU-friendly Locality-Sensitive Hashing (LSH) algorithm [11, 25] as the default clustering algorithm. LSH leverages hash collisions to form different spatial groups. We define the hash function as follows:

$$h_i(x_i) = 1 \text{ if } \beta_i \cdot x_i \geq 0 \text{ else } 0, \quad (4)$$

where \cdot denotes the dot product and $x_i, \beta_i \in \mathbb{R}^d$ are the feature vector and the pre-defined norm vector, respectively. To divide all feature vectors into four groups for example, we randomly initialize two norm vectors β_1, β_2 , and we assign each vector x_i to a hash value:

$$H(x) = h_1(x) + 2h_2(x) \in \{0, 1, 2, 3\}. \quad (5)$$

This LSH scheme is efficient to implement on GPU in a batch of vectors mechanism. It is worth noting that we are not the first to use the LSH algorithm to improve the Transformer block. Reformer [25] replaces the dot-product attention with the fast LSH, reducing the complexity from $O(L^2)$ to $O(L \log L)$ where L is the length of the sequence. Compared to our method, Reformer is applied to the NLP tasks while our work focuses on vision tasks. Furthermore, Reformer [25] still computes the dot-product attention inside the local groups, while DualFormer completely discards the dot-product attention mechanism, resulting in faster training and inference speed with less loss of accuracy.

Intra-Partition Attention. Let $\mathcal{I} = \{I_k\}_{k=1}^K$ denote the clustered partition coordinates generated by the above partition generator. The intra-partition attention weight on the location i which belongs to the cluster I_k is defined as follows:

$$w_i = \frac{x_i}{\sum_{j \in I_k} x_j} \quad (6)$$

where x_i represents the input feature at location i . To obtain the transformed input feature map $\tilde{x} \in \mathbb{R}^{n \times d}$, we use an additional lightweight linear layer. The intra-partition attention feature x^{intra} after communication within each partition is then calculated as:

$$x_i^{intra} = \frac{w_i \cdot \tilde{x}_i}{\sum_{j \in I_k} w_j} \quad (7)$$

Inter-Partition Attention. In addition to capturing intra-partition interactions, inter-partition attention enables the modeling of long-range dependencies by achieving spatial interaction across each partition. To obtain the global descriptor $x^{global} \in \mathbb{R}^{K \times d}$ of all partitions, we use an average pooling operation by computing the mean of all the tokens in each cluster I_k :

$$x_k^{global} = \frac{1}{l_k} \sum_{i \in I_k} \tilde{x}_i \quad (8)$$

Here, l_k represents the number of tokens in cluster I_k . To achieve partition-level interactions, we predict the important coefficients $m \in \mathbb{R}^K$ for each partition, similar to the approach used in SENet [20]. Finally, we compute the inter-partition interaction feature $x^{inter} \in \mathbb{R}^{K \times d}$ as follows:

$$x_k^{inter} = x_k^{global} \cdot \frac{m_k}{\sum_{j \in I_k} m_j} \quad (9)$$

Here, x_k^{inter} represents the interaction feature of the k^{th} partition, x_k^{global} is the global descriptor of k^{th} partition, and m_k is the predicted importance coefficient for the k^{th} partition. The normalization term $\sum_{j \in I_k} m_j$ ensures that the sum of all importance coefficients across all partitions is equal to 1.

Global-to-Local Aggregation. To address the shape misalignment between intra-attention and inter-attention features, we first scatter the inter-partition interaction feature $x^{inter} \in \mathbb{R}^{K \times d}$ to $x^{intra} \in \mathbb{R}^{n \times d}$ based on the clustered groups $\mathcal{C} = \{\mathcal{C}_k\}_{k=1}^K$. After this, we aggregate the inter-attention feature x^{intra} and x^{inter} through concatenation to enhance global-wise dependencies, followed by a simple convolution layer.

Channel to Spatial. To reduce the computational cost, we downsample the input resolution as early stage from $H_i \times W_i \times D_i$ to $\frac{H_i}{k} \times \frac{W_i}{k} \times D_i$, where k is the downsample rate. To recover the original spatial resolution, we use a 1×1 convolution to increase channel dimension from D_i

MPViT	#Layers	Channels	Param.	GFLOPs
Tiny (T)	[2, 2, 4, 2]	[64, 128, 256, 320]	5.5M	1.3
XSmall (XS)	[2, 2, 4, 2]	[64, 128, 320, 368]	10.5M	2.3
Small (S)	[4, 4, 7, 3]	[64, 128, 320, 512]	22.6M	4.4
Base (B)	[6, 12, 25, 7]	[64, 128, 368, 560]	74.0M	15.8

Table 1. **DualFormer Configurations.** #Layers and Channels denote the number of transformer encoders and the embedding dimension in each stage, respectively. FLOPs are measured using 224×224 input image.

to $D_i \times k \times k$. The resulting tensor is then reshaped from $\frac{H_i}{k} \times \frac{W_i}{k} \times (D_i \times k \times k)$ to $H_i \times W_i \times D_i$. Additionally, we use a skip-connection with the original input features to preserve important details and avoid significant loss of information.

3.3. Dual-Attention Transformer

While many studies have focused on combining convolution and attention, few have investigated whether to stack convolution and attention blocks in a serial or parallel way. MaxViT [44] proposes to stack MBCConv, block, and grid attention serially, while UniFormer [28] replaces the attention in the shadow layers with convolution. Meanwhile, the multi-path structure allows for capturing different scales and receptive field attention, which has been successful in downstream tasks [46]. Therefore, we revisit the design mechanism of combining convolution and attention within each block and propose to stack them in parallel.

We implement our proposed dual attention block as a basic build block, similar to MSAs in the vanilla Transformer. As shown in Fig 3, our dual-attention transformer block consists of a convolution block and a multi-head partition attention block. We adopt MBCConv as the default convolution. The convolution block is composed of a 1 convolution and depth-wise convolution, which aims to capture local structure information. The multi-head partition attention block aims to capture global-wise information. For a fair comparison with other ViTs, we build four different network configurations for our Dual-Transformers: DualFormer-T (Tiny), DualFormer-XS (Extra Small), DualFormer-S (Small), and DualFormer-B (Base).

4. Experiments

In this section, we evaluate the proposed DualFormer on three different tasks: image classification on ImageNet [12], semantic segmentation on ADE20K [64], and object detection and instance segmentation on COCO [30]. Additionally, we conduct ablation studies to demonstrate the effectiveness of each component design.

4.1. Image Classification

Dataset. We evaluate our proposed DualFormer on the ImageNet-1K dataset [12], which contains 1.2 million train-

Model	Param.(M)	GFLOPs	Top-1	Reference
DeiT-T [43]	5.7	1.3	72.2	ICML21
XCiT-T12/16 [1]	7.0	1.2	77.1	NeurIPS21
CoaT-Lite T [56]	5.7	1.6	76.6	ICCV21
MPViT-T [27]	5.8	1.6	78.2	CVPR22
DualFormer-T	5.5	1.3	78.4	
ResNet-18 [19]	11.7	1.8	69.8	CVPR16
PVT-T [49]	13.2	1.9	75.1	ICCV21
XCiT-T24/16 [1]	12.0	2.3	79.4	NeurIPS21
CoaT Mi [56]	10.0	6.8	80.8	ICCV21
MPViT-XS [27]	10.5	2.9	80.9	CVPR22
PVT-ACmix-T [36]	13.2	2.0	78.0	CVPR22
DualFormer-XS	10.5	2.3	81.5	
ResNet-50 [19]	25.6	4.1	76.1	CVPR16
PVT-S [49]	24.5	3.8	79.8	ICCV21
DeiT-S/16 [43]	22.1	4.6	79.9	ICML21
Swin-T [31]	29.0	4.5	81.3	ICCV21
CvT-13 [50]	20.0	4.5	81.6	ICCV21
XCiT-S12/16 [1]	26.0	4.8	82.0	NeurIPS21
Focal-T [58]	29.1	4.9	82.2	NeurIPS21
CoaT S [56]	22.0	12.6	82.1	ICCV21
CrossViT-18 [3]	43.3	9.5	82.8	ICCV21
CoaT-Lite S [56]	20.0	4.0	81.9	ICCV21
MPViT-S [27]	22.8	4.7	83.0	CVPR22
iFormer-S [41]	20.0	4.8	83.4	NeurIPS22
DualFormer-S	22.6	4.4	83.5	
ResNeXt-101 [55]	83.5	15.6	79.6	CVPR17
PVT-L [49]	61.4	9.8	81.7	ICCV21
MaxViT-S[44]	69.0	11.7	84.5	ECCV22
DeiT-B/16 [43]	86.6	17.6	81.8	ICML21
XCiT-M24/16 [1]	84.0	16.2	82.7	NeurIPS21
Swin-B [31]	88.0	15.4	83.3	ICCV21
XCiT-S12/8 [1]	26.0	18.9	83.4	NeurIPS21
Focal-B [58]	89.8	16.0	83.8	NeurIPS21
MPViT-B [27]	74.8	16.4	84.3	CVPR22
iFormer-B [41]	87.0	14.0	84.6	NeurIPS22
DualFormer-B	74.0	15.8	84.8	

Table 2. **ImageNet-1K classification.** These models are trained with 224×224 resolution. For fair comparison, we do not include models that are distilled [43] or use 384×384 resolution.

ing images and 50,000 validation images with 1,000 semantic categories. We adopt the AdamW [34] optimizer with an initial learning rate of 5×10^{-4} , momentum of 0.9, and weight decay of 5×10^{-2} . The batch size is 1024, and the default number of epochs is 300, trained on 8 Tesla V100 GPUs. During training, we set the number of linear warm-up and cool-down epochs to 5 and 10, respectively. In other epochs, we decrease the learning rate with a cosine annealing schedule. Following previous work [43], we use data augmentation techniques such as random flipping, mixup [62], and cutmix [61]. We report the Top-1 accuracy under the single crop setting, which is a common evaluation metric. Additionally, we report the model size and the number of floating-point operations to display the trade-off between accuracy and model size.

Results. Table 2 presents the Top-1 accuracy achieved by DualFormer in the image classification task, in comparison to previous state-of-the-art models. Notably, Du-

Backbone	Params. (M)	GFLOPs	Mask R-CNN 1× schedule						Mask R-CNN 3× schedule + MS					
			AP^b	AP_{50}^b	AP_{75}^b	AP^m	AP_{50}^m	AP_{75}^m	AP^b	AP_{50}^b	AP_{75}^b	AP^m	AP_{50}^m	AP_{75}^m
ResNet18 [19]	31	207	34.0	54.0	36.7	31.2	51.0	32.7	36.9	57.1	40.0	33.6	53.9	35.7
PVT-T [49]	33	240	36.7	59.2	39.3	35.1	56.7	37.3	39.8	62.2	43.0	37.4	59.3	39.9
MPViT-T [27]	28	216	42.2	64.2	45.8	39.0	61.4	41.8	44.8	66.9	49.2	41.0	64.2	44.1
DualFormer-T	25	208	42.4	65.0	46.4	39.2	61.6	42.2	45.1	67.3	49.6	41.2	64.3	44.3
ResNet50 [19]	44	260	38.0	58.6	41.4	34.4	55.1	36.7	41.0	61.7	44.9	37.1	58.4	40.1
PVT-S [49]	44	245	40.4	62.9	43.8	37.8	60.1	40.3	43.0	65.3	46.9	39.9	62.5	42.8
Swin-T [31]	48	264	43.7	66.6	47.7	39.8	63.3	42.7	46.0	68.1	50.3	41.6	65.1	44.9
Focal-T [58]	49	291	44.8	67.7	49.2	41.0	64.7	44.2	47.2	69.4	51.9	42.7	66.5	45.9
MPViT-XS [27]	30	231	44.2	66.7	48.4	40.4	63.4	43.4	46.6	68.5	51.1	42.3	65.8	45.8
DualFormer-XS	29	219	44.6	67.1	48.9	40.8	63.9	43.8	47.0	69.0	51.6	42.5	66.1	45.8
ResNet101 [19]	63	336	40.4	61.1	44.2	36.4	57.7	38.8	42.8	63.2	47.1	38.5	60.1	41.3
PVT-M [49]	64	392	42.0	64.4	45.6	39.0	61.6	42.1	44.2	66.0	48.2	40.5	63.1	43.5
Swin-S [31]	69	359	46.5	68.7	51.3	42.1	65.8	45.2	48.5	70.2	53.5	43.3	67.3	46.6
Focal-S [58]	71	401	47.4	69.8	51.9	42.8	66.6	46.1	48.8	70.5	53.6	43.8	67.7	47.2
MPViT-S [27]	43	268	46.4	68.6	51.2	42.4	65.6	45.7	48.4	70.5	52.6	43.9	67.6	47.5
DualFormer-S	43	258	46.8	69.0	51.5	42.6	66.0	45.9	48.6	70.5	52.8	44.0	67.7	47.3
ResNeXt101-64x4d [55]	102	493	42.8	63.8	47.3	38.4	60.6	41.3	44.4	64.9	48.8	39.7	61.9	42.6
PVT-L [49]	81	457	42.9	65.0	46.6	39.5	61.9	42.5	44.5	66.0	48.3	40.7	63.4	43.7
Swin-B [31]	107	496	46.9	69.2	51.6	42.3	66.0	45.5	48.5	69.8	53.2	43.4	66.8	49.6
Focal-B [58]	110	533	47.8	70.2	52.5	43.2	67.3	46.5	49.0	70.1	53.6	43.7	67.6	47.0
MPViT-B [27]	95	503	48.2	70.0	52.9	43.5	67.1	46.8	49.4	70.9	54.3	44.5	68.1	48.2
DualFormer-B	95	495	48.5	70.3	53.0	43.6	67.2	46.9	49.6	71.0	54.5	44.6	68.2	48.4

Table 3. **COCO detection and instance segmentation** with Mask R-CNN [18]. Models are trained for 1× schedule and 3× schedule [51] with multi-scale training inputs (MS) [31, 42]. All backbones are pretrained on ImageNet-1K. For fair comparison, we omit models pretrained on larger-datasets (e.g., ImageNet-21K). The GFLOPs are measured at resolution 800 × 1280.

alFormer outperforms most ConvNets, ViTs, and MLPs with similar parameters and computational costs. For instance, DualFormer-T achieves higher accuracy than the recent MPViT-XS [27] by 0.2%, while using 18.8% fewer FLOPs. Moreover, DualFormer-S demonstrates a significant improvement in Top-1 accuracy, with gains of 1.1% and 2.2% compared to Focal Transformer [58].

4.2. Object Detection

Dataset. We conducted an evaluation of DualFormer on the COCO 2017 benchmark [30] for both object detection and instance segmentation tasks. The COCO 2017 dataset comprises 118K train images and 5k validation images. To ensure a fair comparison, we followed the train and validation recipe of PVT [49] for both object detection and instance segmentation. The backbone was pre-trained on ImageNet-1k, and the training was performed using a batch size of 16 on 8 Tesla V100 GPUs. The number of training epochs was set to 12 and 36 (1× schedule), following the methodology of previous works [18, 31, 27].

Results. Table 3 presents the results of our evaluation of COCO 2017 using Mask R-CNN. Our DualFormer model outperforms pure ConvNets such as ResNet [19], as well as Transformer variants PVT [49] and Swin Transformer [31] across all metrics. Notably, DualFormer-S consistently outperforms Swin-T [31] by approximately 0.9% in box AP and 1.0% in mask AP of Mask R-CNN under 1× evaluation, while using significantly fewer parameters and FLOPs.

Backbone	Params.	GFLOPs	mIoU
Swin-T [31]	59M	945	44.5
Focal-T [58]	62M	998	45.8
XCiT-S12/16 [1]	54M	966	45.9
XCiT-S12/8 [1]	53M	1237	46.6
MPViT-S [27]	52M	943	48.3
iFormer-S [41]	49M	938	48.4
DualFormer-S	48M	922	48.6
ResNet-101 [19]	85M	1029	43.8
XCiT-S24/16 [1]	76M	1053	46.9
Swin-S [31]	81M	1038	47.6
XCiT-M24/16 [1]	112M	1213	47.6
Focal-S [58]	85M	1130	48.0
Swin-B [31]	121M	1841	48.1
XCiT-S24/8 [1]	74M	1587	48.1
XCiT-M24/8 [1]	110M	2161	48.4
Focal-B [58]	126M	1354	49.0
MPViT-B [27]	105M	1186	50.3
DualFormer-B	104M	1150	50.5

Table 4. **ADE20k semantic segmentation** results using UperNet [53]. GFLOPs are calculated with resolution 512 × 2048. For a fair comparison, We do not include models that are pre-trained on larger datasets (i.e., ImageNet-21K).

4.3. Semantic Segmentation

Dataset. The ADE20K [64] dataset is a widely used benchmark for semantic segmentation, comprising 150 object and stuff classes and diverse scene annotations. The dataset includes 20K images in the training set and 2k images in the validation set. To conduct our experiments, we utilized the MMSegmentation [4] toolbox [7] as our codebase. To en-

Parallel	Depth-wise	Intra	Inter	Top-1 Acc
✓	✗	✓	✗	80.6
✓	✗	✗	✓	80.8
✓	✗	✓	✓	81.2
✗	✓	✓	✓	81.0
✓	✓	✓	✓	81.5

Table 5. Ablation study on each component of DualFormer block. We report Top-1 accuracy based on DualFormer-XS. Intra and Inter mean intra-partition and inter-partition attention, respectively.

sure a fair comparison, we followed the training and validation recipe of PVT [49] for semantic segmentation experiments. We employed UperNet [53] as the segmentation head, and the backbones were initialized with weights pre-trained on ImageNet-1K. To optimize our model, we utilized an AdamW [34] optimizer with an initial learning rate of 10^{-4} and weight decay of 10^{-4} . The training was performed using a batch size of 32 on 8 Tesla V100 GPUs, and a total of 80K iterations were trained.

Results. Table 4 displays the results of our evaluation on the UperNet model for semantic segmentation. Our DualFormer model achieves stable performance gains over MPViT [27], which incorporates a multi-path branch for architecture design. Notably, with approximately 50M parameters, DualFormer-S outperforms MPViT-S by 0.3% in mIoU. Furthermore, compared to the recent work iFormer [41], DualFormer-S surpasses iFormer-S by 0.2% in mIoU while using fewer parameters and FLOPs, demonstrating the effectiveness of DualFormer’s design.

4.4. Ablation Study

Effectiveness of each component. To demonstrate the effectiveness of each component, we conducted ablation studies on the ImageNet-1k dataset, and the results of DualFormer-XS are presented in Table 5. In this table, *Parallel* refers to the stacking way of the convolution and self-attention, *Intra* refers to the proposed intra-partition attention module, *Inter* refers to the proposed inter-partition attention module, and *Depth-wise* means whether using the depth-wise convolution of local feature extractor. We achieved an accuracy of 80.6% with only the intra-partition attention. This accuracy further improved to 81.2% when combining the intra- and inter-partition attention, demonstrating the effectiveness of long-range information interaction. When equipped with the depth-wise convolution branch, i.e., MBCConv, DualFormer-XS achieved an accuracy of 81.5%, obtaining a 0.3% accuracy gain, which indicates the effectiveness of the convolution branch.

Different Clustering Methods. We conduct an ablation experiment to study the influence of different clustering methods, which is shown in Table 6. Both methods promote the baseline significantly. Compared with LSH [11], K-Means [32] further increases the accuracy by a slight margin

of 0.1%, but with extreme speed drops. Therefore, we adopt LSH to strike an ideal balance between speed and accuracy.

Method	Throughput	Param	GFLOPs	Top-1
MPViT-XS	640	10.9	2.5	80.9
K-Means	806	10.5	2.3	81.6
LSH	1253	10.5	2.3	81.5

Table 6. Comparison of different clustering methods with MPViT-XS. The results are based on DualFormer-XS. We report throughput and Top-1 accuracy on the ImageNet-1K validation set.

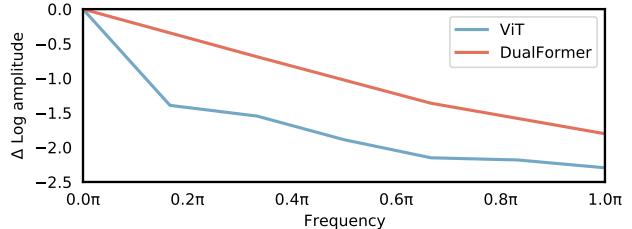


Figure 5. Comparison of relative log amplitudes of Fourier transformed feature maps for ViT and DualFormer.

Fourier Analysis. To exploit why dual-attention block works, we conduct visualization from a Fourier analysis following previous work [37], which is shown in Fig 5. The results indicate that DualFormer has a greater amplitude at higher frequencies compared to vanilla ViT. This finding supports the hypothesis that DualFormer can capture more high-frequency information, which in turn helps to generate more robust and discriminative feature representations.

Stacking convolution and self-attention in parallel or in series? To explore the effective way of combining self-attention and convolution, we also implemented a stacking in-series approach, which is shown in Table 5. However, changing from the parallel approach to the series approach resulted in a 0.5% Top-1 accuracy drop, indicating the effectiveness of the parallel approach. Additionally, compared with the recent stage-wise parallel approach MPViT as shown in Table 6, DualFormer excels both in accuracy and efficiency.

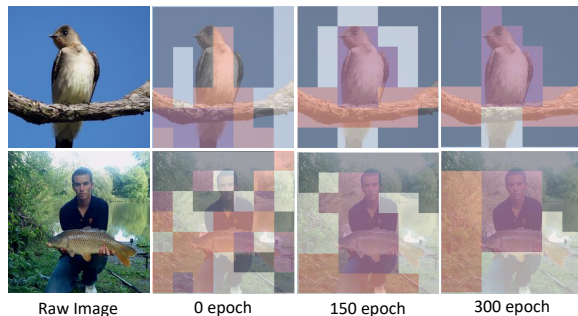


Figure 6. Visualization of the partition result at different training epochs. Raw images are taken from ImageNet-1K validation set.

Partition Visualization. To qualitatively analyze whether the clustering operation forms semantically meaningful

groups, we visualized the partition results of three training periods, i.e., 0, 150, and 300 epochs. As shown in Fig 6, the grouping process becomes more rational as the training epochs increase. The semantically similar positions are grouped together. For instance, in the first row of Fig 6, the grouping process initially appears nonsensical. However, as the training progresses, the body of the bird is well-clustered into the purple group at 150 epochs, despite the white group wrongly classifying the tail of the bird as tokens of the sky. Ultimately, at 300 epochs, the positions of the tail are successfully separated into a new group. These results demonstrate that DualFormer is capable of capturing reasonable feature representations at different positions.

5. Conclusion

In this paper, we propose to combine convolution and attention in parallel to adaptively capture different scales and receptive field information, which is seldom adopted by previous works. To address the issue of spatial redundancy in vanilla self-attention, we introduce a clustering scheme to approximate the self-attention mechanism. The scheme involves partitioning the feature maps using local sensitivity hashing and computing the proxy features of each group. We then activate these proxy features through a global-wise interaction mechanism and distribute them to the corresponding query positions. Based on the proposed dual-attention block, we present DualFormer, which achieves state-of-the-art performance on various tasks including image classification, object detection, and semantic segmentation. We hope that our approach will inspire further research on effective and efficient ways of combining convolution and attention.

References

- [1] Alaaeldin Ali, Hugo Touvron, Mathilde Caron, Piotr Bojanowski, Matthijs Douze, Armand Joulin, Ivan Laptev, Natalia Neverova, Gabriel Synnaeve, Jakob Verbeek, et al. Xcit: Cross-covariance image transformers. *Advances in Neural Information Processing Systems*, 34, 2021.
- [2] Yue Cao, Jiarui Xu, Stephen Lin, Fangyun Wei, and Han Hu. Gcnet: Non-local networks meet squeeze-excitation networks and beyond. In *IEEE International Conference on Computer Vision workshops*, pages 0–0, 2019.
- [3] Chun-Fu Richard Chen, Quanfu Fan, and Rameswar Panda. Crossvit: Cross-attention multi-scale vision transformer for image classification. In *Proceedings of the IEEE International Conference on Computer Vision*, pages 357–366, 2021.
- [4] Kai Chen, Jiaqi Wang, Jiangmiao Pang, Yuhang Cao, Yu Xiong, Xiaoxiao Li, Shuyang Sun, Wansen Feng, Ziwei Liu, Jiarui Xu, et al. Mmdetection: Open mmlab detection toolbox and benchmark. *arXiv preprint arXiv:1906.07155*, 2019.
- [5] Liang-Chieh Chen, George Papandreou, Iasonas Kokkinos, Kevin Murphy, and Alan L Yuille. Deeplab: Semantic image segmentation with deep convolutional nets, atrous convolution, and fully connected crfs. *IEEE Transactions on Pattern Analysis and Machine Intelligence*, 40(4):834–848, 2017.
- [6] Krzysztof Choromanski, Valerii Likhoshesterov, David Dohan, Xingyou Song, Andreea Gane, Tamas Sarlos, Peter Hawkins, Jared Davis, Afroz Mohiuddin, Lukasz Kaiser, et al. Rethinking attention with performers. *arXiv preprint arXiv:2009.14794*, 2020.
- [7] MMSegmentation Contributors. MMSegmentation: Openmmlab semantic segmentation toolbox and benchmark. <https://github.com/open-mmlab/mms Segmentation>, 2020.
- [8] Jifeng Dai, Yi Li, Kaiming He, and Jian Sun. R-fcn: Object detection via region-based fully convolutional networks. *Advances in Neural Information Processing Systems*, 29, 2016.
- [9] Zihang Dai, Hanxiao Liu, Quoc V Le, and Mingxing Tan. Coatnet: Marrying convolution and attention for all data sizes. *Advances in Neural Information Processing Systems*, 34, 2021.
- [10] Tri Dao, Daniel Y Fu, Stefano Ermon, Atri Rudra, and Christopher Ré. Flashattention: Fast and memory-efficient exact attention with io-awareness. *arXiv preprint arXiv:2205.14135*, 2022.
- [11] Anirban Dasgupta, Ravi Kumar, and Tamás Sarlós. Fast locality-sensitive hashing. In *Proceedings of the 17th ACM SIGKDD International Conference on Knowledge Discovery and Data Mining*, pages 1073–1081, 2011.
- [12] Jia Deng, Wei Dong, Richard Socher, Li-Jia Li, Kai Li, and Li Fei-Fei. Imagenet: A large-scale hierarchical image database. In *IEEE Conference on Computer Vision and Pattern Recognition*, pages 248–255, 2009.
- [13] Xiaoyi Dong, Jianmin Bao, Dongdong Chen, Weiming Zhang, Nenghai Yu, Lu Yuan, Dong Chen, and Baining Guo. Cswin transformer: A general vision transformer backbone with cross-shaped windows. In *IEEE Conference on Computer Vision and Pattern Recognition*, pages 12124–12134, 2022.
- [14] Alexey Dosovitskiy, Lucas Beyer, Alexander Kolesnikov, Dirk Weissenborn, Xiaohua Zhai, Thomas Unterthiner, Mostafa Dehghani, Matthias Minderer, Georg Heigold, Sylvain Gelly, et al. An image is worth 16x16 words: Transformers for image recognition at scale. *arXiv preprint arXiv:2010.11929*, 2020.
- [15] Peng Gao, Jiasen Lu, Hongsheng Li, Roozbeh Mottaghi, and Aniruddha Kembhavi. Container: Context aggregation network. *arXiv preprint arXiv:2106.01401*, 2021.
- [16] Zhengyang Geng, Meng-Hao Guo, Hongxu Chen, Xia Li, Ke Wei, and Zhouchen Lin. Is attention better than matrix decomposition? *arXiv preprint arXiv:2109.04553*, 2021.
- [17] Jianyuan Guo, Kai Han, Han Wu, Yehui Tang, Xinghao Chen, Yunhe Wang, and Chang Xu. Cmt: Convolutional neural networks meet vision transformers. In *IEEE Conference on Computer Vision and Pattern Recognition*, pages 12175–12185, 2022.
- [18] Kaiming He, Georgia Gkioxari, Piotr Dollár, and Ross Girshick. Mask r-cnn. In *IEEE International Conference on Computer Vision*, pages 2961–2969, 2017.

- [19] Kaiming He, Xiangyu Zhang, Shaoqing Ren, and Jian Sun. Deep residual learning for image recognition. In *IEEE Conference on Computer Vision and Pattern Recognition*, pages 770–778, 2016.
- [20] Jie Hu, Li Shen, and Gang Sun. Squeeze-and-excitation networks. In *IEEE Conference on Computer Vision and Pattern Recognition*, pages 7132–7141, 2018.
- [21] Zhengkai Jiang, Peng Gao, Chaoxu Guo, Qian Zhang, Shiming Xiang, and Chunhong Pan. Video object detection with locally-weighted deformable neighbors. In *Proceedings of the AAAI Conference on Artificial Intelligence*, volume 33, pages 8529–8536, 2019.
- [22] Zhengkai Jiang, Zhangxuan Gu, Jinlong Peng, Hang Zhou, Liang Liu, Yabiao Wang, Ying Tai, Chengjie Wang, and Liqing Zhang. Stc: spatio-temporal contrastive learning for video instance segmentation. In *European Conference on Computer Vision*, pages 539–556. Springer, 2023.
- [23] Zhengkai Jiang, Yuxi Li, Ceyuan Yang, Peng Gao, Yabiao Wang, Ying Tai, and Chengjie Wang. Prototypical contrast adaptation for domain adaptive semantic segmentation. In *European Conference on Computer Vision*, pages 36–54. Springer, 2022.
- [24] Zhengkai Jiang, Yu Liu, Ceyuan Yang, Jihao Liu, Peng Gao, Qian Zhang, Shiming Xiang, and Chunhong Pan. Learning where to focus for efficient video object detection. In *European Conference on Computer Vision*, pages 18–34. Springer, 2020.
- [25] Nikita Kitaev, Łukasz Kaiser, and Anselm Levskaya. Reformer: The efficient transformer. *arXiv preprint arXiv:2001.04451*, 2020.
- [26] Alex Krizhevsky, Ilya Sutskever, and Geoffrey E Hinton. Imagenet classification with deep convolutional neural networks. *Advances in Neural Information Processing Systems*, 25, 2012.
- [27] Youngwan Lee, Jonghee Kim, Jeffrey Willette, and Sung Ju Hwang. Mpvit: Multi-path vision transformer for dense prediction. In *IEEE Conference on Computer Vision and Pattern Recognition*, 2022.
- [28] Kunchang Li, Yali Wang, Peng Gao, Guanglu Song, Yu Liu, Hongsheng Li, and Yu Qiao. Uniformer: Unified transformer for efficient spatiotemporal representation learning. *arXiv preprint arXiv:2201.04676*, 2022.
- [29] Tsung-Yi Lin, Piotr Dollár, Ross Girshick, Kaiming He, Bharath Hariharan, and Serge Belongie. Feature pyramid networks for object detection. In *IEEE Conference on Computer Vision and Pattern Recognition*, pages 2117–2125, 2017.
- [30] Tsung-Yi Lin, Michael Maire, Serge Belongie, James Hays, Pietro Perona, Deva Ramanan, Piotr Dollár, and C Lawrence Zitnick. Microsoft coco: Common objects in context. In *European Conference on Computer Vision*, pages 740–755, 2014.
- [31] Ze Liu, Yutong Lin, Yue Cao, Han Hu, Yixuan Wei, Zheng Zhang, Stephen Lin, and Baining Guo. Swin transformer: Hierarchical vision transformer using shifted windows. In *IEEE International Conference on Computer Vision*, pages 10012–10022, 2021.
- [32] Stuart Lloyd. Least squares quantization in pcm. *IEEE Transactions on Information Theory*, 28(2):129–137, 1982.
- [33] Jonathan Long, Evan Shelhamer, and Trevor Darrell. Fully convolutional networks for semantic segmentation. In *IEEE Conference on Computer Vision and Pattern Recognition*, pages 3431–3440, 2015.
- [34] Ilya Loshchilov and Frank Hutter. Decoupled weight decay regularization. *arXiv preprint arXiv:1711.05101*, 2017.
- [35] Jiachen Lu, Jinghan Yao, Junge Zhang, Xiatian Zhu, Hang Xu, Weiguo Gao, Chunjing Xu, Tao Xiang, and Li Zhang. Soft: softmax-free transformer with linear complexity. *Advances in Neural Information Processing Systems*, 34:21297–21309, 2021.
- [36] Xuran Pan, Chunjiang Ge, Rui Lu, Shiji Song, Guanfu Chen, Zeyi Huang, and Gao Huang. On the integration of self-attention and convolution. In *IEEE Conference on Computer Vision and Pattern Recognition*, pages 815–825, 2022.
- [37] Namuk Park and Songkuk Kim. How do vision transformers work? *arXiv preprint arXiv:2202.06709*, 2022.
- [38] Shaoqing Ren, Kaiming He, Ross Girshick, and Jian Sun. Faster r-cnn: Towards real-time object detection with region proposal networks. *Advances in Neural Information Processing Systems*, 28, 2015.
- [39] Mark Sandler, Andrew Howard, Menglong Zhu, Andrey Zhmoginov, and Liang-Chieh Chen. Mobilenetv2: Inverted residuals and linear bottlenecks. In *Proceedings of the IEEE Conference on Computer Vision and Pattern Recognition*, pages 4510–4520, 2018.
- [40] Zhuoran Shen, Mingyuan Zhang, Haiyu Zhao, Shuai Yi, and Hongsheng Li. Efficient attention: Attention with linear complexities. In *IEEE Winter Conference on Applications of Computer Vision*, pages 3531–3539, 2021.
- [41] Chenyang Si, Weihao Yu, Pan Zhou, Yichen Zhou, Xinchao Wang, and Shuicheng Yan. Inception transformer. *arXiv preprint arXiv:2205.12956*, 2022.
- [42] Peize Sun, Rufeng Zhang, Yi Jiang, Tao Kong, Chenfeng Xu, Wei Zhan, Masayoshi Tomizuka, Lei Li, Zehuan Yuan, Changhu Wang, et al. Sparse r-cnn: End-to-end object detection with learnable proposals. In *Proceedings of the IEEE Conference on Computer Vision and Pattern Recognition*, pages 14454–14463, 2021.
- [43] Hugo Touvron, Matthieu Cord, Matthijs Douze, Francisco Massa, Alexandre Sablayrolles, and Hervé Jégou. Training data-efficient image transformers & distillation through attention. In *International Conference on Machine Learning*, pages 10347–10357. PMLR, 2021.
- [44] Zhengzhong Tu, Hossein Talebi, Han Zhang, Feng Yang, Peyman Milanfar, Alan Bovik, and Yinxiao Li. Maxvit: Multi-axis vision transformer. *arXiv preprint arXiv:2204.01697*, 2022.
- [45] Ashish Vaswani, Noam Shazeer, Niki Parmar, Jakob Uszkoreit, Llion Jones, Aidan N Gomez, Łukasz Kaiser, and Illia Polosukhin. Attention is all you need. *Advances in Neural Information Processing Systems*, 30, 2017.
- [46] Haohan Wang, Xindi Wu, Zeyi Huang, and Eric P Xing. High-frequency component helps explain the generalization of convolutional neural networks. In *IEEE Conference*

- on *Computer Vision and Pattern Recognition*, pages 8684–8694, 2020.
- [47] Jingdong Wang, Ke Sun, Tianheng Cheng, Borui Jiang, Chaorui Deng, Yang Zhao, Dong Liu, Yadong Mu, Mingkui Tan, Xinggang Wang, et al. Deep high-resolution representation learning for visual recognition. *IEEE Transactions on Pattern Analysis and Machine Intelligence*, 43(10):3349–3364, 2020.
- [48] Wenhai Wang, Enze Xie, Xiang Li, Deng-Ping Fan, Kaitao Song, Ding Liang, Tong Lu, Ping Luo, and Ling Shao. Pvtv2: Improved baselines with pyramid vision transformer. *arXiv preprint arXiv:2106.13797*, 2021.
- [49] Wenhai Wang, Enze Xie, Xiang Li, Deng-Ping Fan, Kaitao Song, Ding Liang, Tong Lu, Ping Luo, and Ling Shao. Pyramid vision transformer: A versatile backbone for dense prediction without convolutions. In *IEEE International Conference on Computer Vision*, pages 568–578, 2021.
- [50] Haiping Wu, Bin Xiao, Noel Codella, Mengchen Liu, Xiyang Dai, Lu Yuan, and Lei Zhang. Cvt: Introducing convolutions to vision transformers. In *IEEE International Conference on Computer Vision*, pages 22–31, 2021.
- [51] Yuxin Wu, Alexander Kirillov, Francisco Massa, Wan-Yen Lo, and Ross Girshick. Detectron2. <https://github.com/facebookresearch/detectron2>, 2019.
- [52] Zhuofan Xia, Xuran Pan, Shiji Song, Li Erran Li, and Gao Huang. Vision transformer with deformable attention. In *Proceedings of the IEEE Conference on Computer Vision and Pattern Recognition*, pages 4794–4803, 2022.
- [53] Tete Xiao, Yingcheng Liu, Bolei Zhou, Yuning Jiang, and Jian Sun. Unified perceptual parsing for scene understanding. In *Proceedings of the European Conference on Computer Vision*, pages 418–434, 2018.
- [54] Tete Xiao, Mannat Singh, Eric Mintun, Trevor Darrell, Piotr Dollár, and Ross Girshick. Early convolutions help transformers see better. *Advances in Neural Information Processing Systems*, 34, 2021.
- [55] Saining Xie, Ross Girshick, Piotr Dollár, Zhuowen Tu, and Kaiming He. Aggregated residual transformations for deep neural networks. In *IEEE Conference on Computer Vision and Pattern Recognition*, pages 1492–1500, 2017.
- [56] Weijian Xu, Yifan Xu, Tyler Chang, and Zhuowen Tu. Co-scale conv-attentional image transformers. In *Proceedings of the IEEE International Conference on Computer Vision*, pages 9981–9990, 2021.
- [57] Chenglin Yang, Siyuan Qiao, Qihang Yu, Xiaoding Yuan, Yukun Zhu, Alan Yuille, Hartwig Adam, and Liang-Chieh Chen. Moat: Alternating mobile convolution and attention brings strong vision models. *arXiv preprint arXiv:2210.01820*, 2022.
- [58] Jianwei Yang, Chunyuan Li, Pengchuan Zhang, Xiyang Dai, Bin Xiao, Lu Yuan, and Jianfeng Gao. Focal self-attention for local-global interactions in vision transformers. *arXiv preprint arXiv:2107.00641*, 2021.
- [59] Weihao Yu, Mi Luo, Pan Zhou, Chenyang Si, Yichen Zhou, Xinchao Wang, Jiashi Feng, and Shuicheng Yan. Metaformer is actually what you need for vision. In *IEEE Conference on Computer Vision and Pattern Recognition*, pages 10819–10829, 2022.
- [60] Kun Yuan, Shaopeng Guo, Ziwei Liu, Aojun Zhou, Fengwei Yu, and Wei Wu. Incorporating convolution designs into visual transformers. In *IEEE International Conference on Computer Vision*, pages 579–588, 2021.
- [61] Sangdoon Yun, Dongyoon Han, Seong Joon Oh, Sanghyuk Chun, Junsuk Choe, and Youngjoon Yoo. Cutmix: Regularization strategy to train strong classifiers with localizable features. In *IEEE International Conference on Computer Vision*, pages 6023–6032, 2019.
- [62] Hongyi Zhang, Moustapha Cisse, Yann N Dauphin, and David Lopez-Paz. mixup: Beyond empirical risk minimization. In *International Conference on Learning Representations*, 2018.
- [63] Qiming Zhang, Yufei Xu, Jing Zhang, and Dacheng Tao. Vitaev2: Vision transformer advanced by exploring inductive bias for image recognition and beyond. *International Journal of Computer Vision*, pages 1–22, 2023.
- [64] Bolei Zhou, Hang Zhao, Xavier Puig, Tete Xiao, Sanja Fidler, Adela Barriuso, and Antonio Torralba. Semantic understanding of scenes through the ade20k dataset. *International Journal of Computer Vision*, 127(3):302–321, 2019.